Interconnect Estimation for Mesh-Based Reconfigurable Computing

Haibin Shen, Rongquan You, Yier Jin, and Aiming Ji

Institute of VLSI Design, Zhejiang University,
Hangzhou, P.R. China
{shb,yourq,jinye,jiam}@vlsi.zju.edu.cn

Abstract. The paper presents a new stochastic model for mesh-based reconfigurable computing. Under the conditions of several statistical assumptions, closed formulae of probability and mathematical expectation are derived for each type of connections. Both the theoretical deduction and simulation results are given to verify our approach. The elementary research can be applied to implement and optimize the interconnect resource of mesh-based reconfigurable computing.

keywords: Interconnect, reconfigurable computing, mesh-based, probability

1 Introduction

Reconfigurable computing is emerging as the new paradigm for satisfying the simultaneous demand for application performance and flexibility [8]. Thus, Many applications have been mapped onto reconfigurable architectures [2,9,10,11,12]. These applications include object recognition, image filtering, fingerprint matching, image compression, and stereo vision, and many applications have been demonstrated to have superior performance on reconfigurable architectures compared to other existing architectures [8].

A very attractive interconnection scheme is the mesh-connected computer because of its simplicity, regularity, and the fact that the interconnections occupy only a fixed fraction of the area no matter how large the chip [3,6]. Mesh-based reconfigurable computing (MBRC) is realized by a processing element (PE) array, and the design of PE includes operators and interconnections. Although rich interconnect resource can provide high flexible interconnect ability, it increases the area and power of the array. Formerly, the interconnect space exploration of reconfigurable computing is mostly accomplished by analyzing and comparing, which is not precise enough [6]. In related research, a typical estimation for the interconnections in gate arrays has been presented in [5], and following research has worked out more precise results, which can estimate the channel width, the routablity and the wire length [3, 7, 14]. Because the interconnections of MBRC are different from those of gate array, the models for the latter one are not suitable for the former one. In this paper, elementary research on interconnect estimation of MBRC is presented.

The organization of this paper is as follows. In Section 2, we define the interconnect resource. Section 3 provides an overview of the stochastic model and proposes the main statistical assumptions. The task of estimating the probabilities of interconnections and their mathematical expectations is the subject of Section 4. The comparison of theoretical estimation and simulation results is given in Section 5. Section 6 serves as the conclusion.

2 Interconnect Resource

The interconnect resource of mesh-based reconfigurable computing belongs to PEs, and many PEs constitute a PE array as Fig. 1.

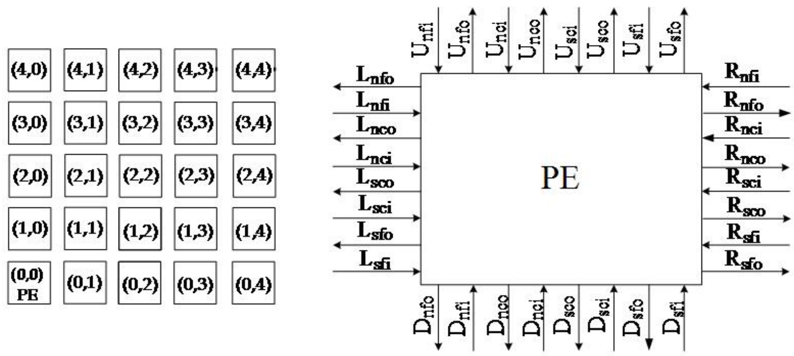

Fig. 1. Interconnect model of reconfigurable processing element array

In Fig. 1, the interconnect resource of a PE includes four borders of it, which are denoted as U, D, L and R, and the types of connections are classified as follows:

(1) Connections among PEs. "*i*" , "*o*", "*n*" and "*s*" denote "input", "output", "nearest neighbour" and "hop neighbour" respectively, in which "nearest neighbour" means the connection can only be connected to the nearest PE with the length of 1 unit (e.g. the connection length between PE$(0, 0)$ and PE(0, 1) is 1 unit), and "hop neighbour" means the connection can only be connected to the PE which is at the same row or column with the length of w units.

(2) Connections in PEs. "f" and "c" denote "function connections" and "channel connections", in which the former ones mean the connections are connected to the operators in PEs, serving as the inputs or outputs of the operators, and the latter ones mean the connections are not connected to the operators, but traverse from one border to another of a PE. Function connections and channel connections are implemented by using multiplexors in PEs.

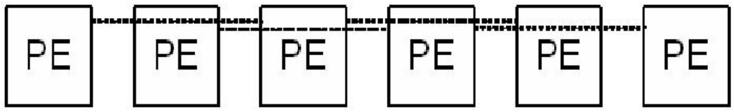

Fig. 2. Hop neighbour connections with $w = 2$

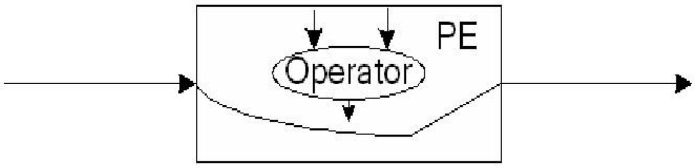

Fig. 3. Function connections and channel connections in a PE

3 Stochastic Model

It is assumed that the number of connections per PE can be drawn independently from a Poisson distribution with parameter λ, where λ is defined as the quotient of the number of connections in a circuit divided by the number of PEs in the array [1]. Because each border of a PE is equivalent, the number of connections per border of a PE can be drawn independently from a Poisson distribution with parameter $\lambda/4$. It is further assumed that connection length L is independently chosen according to a geometric distribution $G(L) = (1-\varepsilon)\varepsilon^{L-1}$, where $0 < \varepsilon < 1$ [1].

Different from other networks, the connections of PEs are directional. Assume x_1 is a connection starting from PE(a, b) and ending at PE(u, v), our stochastic model always chooses the path with the minimal Manhattan distance $L = |u - a| + |v - b|$, and chooses hop neighbour connection if possible. Thus, there are $C_L^{|u-a|} (= C_L^{|v-b|})$ possible paths from PE(a, b) to PE(u, v). When PE(u, v) is at the same row or column with PE(a, b), x_1 can only choose one border of PE(u, v), otherwise x_1 can choose two borders of it. On the other hand, a connection x_2 drawn from PE(a, b) with length L, can end at $4L$ possible PEs. Therefore, x_2 can end at $(8L - 4)$ possible borders in the PE array. Assume that x_2 chooses one border out of the $(8L - 4)$ possible borders with the same probability, the probability of choosing each border is $q(L) = \frac{1}{8L-4}$.

4 Probabilities of Connections

Lemma 1: For a connection x_3, emanating from the upper border of PE$(0, 0)$ and terminating at PE(r, s), the probabilities of the events that x_3 uses U_{nfo}

and U_{sfo} of PE$(0,0)$ are $P(U_{nfo})$ and $P(U_{sfo})$, respectively:

$$P(U_{nfo}) = \sum_{L=1}^{\infty} G(L) \frac{\sum_{s=-L+1}^{L-1} C_{L-1}^{|s|}}{\sum_{s=-L+1}^{L-1} C_{L-1}^{|s|} + \sum_{s=-L+w}^{L-w} C_{L-w}^{|s|}} \quad (1)$$

$$P(U_{sfo}) = \sum_{L=1}^{\infty} G(L) \frac{\sum_{s=-L+w}^{L-w} C_{L-w}^{|s|}}{\sum_{s=-L+1}^{L-1} C_{L-1}^{|s|} + \sum_{s=-L+w}^{L-w} C_{L-w}^{|s|}} \quad (2)$$

where, $L = |r| + |s|$, the length of hop neighbour connection $w > 1$, and $C_0^0 = 1$. When $L < w$, $C_{L-w}^{|s|} = 0$

Proof: As Fig. 1, if x_3 uses U_{nfo} of PE$(0,0)$, it will pass through PE$(1,0)$, and there are $C_{L-1}^{|s|}$ possible paths from PE$(1,0)$ to PE(r,s). Because our stochastic model always chooses the path with the minimal Manhattan distance, PE(r,s) should be above the dash in Fig. 4. Thus, there are $\sum_{s=-L+1}^{L-1} C_{L-1}^{|s|}$ possible paths for x_3 with length L. Similarly, if x_3 uses U_{sfo} of PE$(0,0)$, it will pass through PE$(w,0)$, and then PE(r,s) should be above the dashdot in Fig. 4. Thereby, there are $C_{L-w}^{|s|}$ possible paths from PE(r,s) to PE$(w,0)$, and there are $\sum_{s=-L+w}^{L-w} C_{L-w}^{|s|}$ possible paths for x_3 with length L.

Among the connections starting from the upper border of PE$(0,0)$ with length L, the proportion of using U_{nfo} is $\frac{\sum_{s=-L+1}^{L-1} C_{L-1}^{|s|}}{\sum_{s=-L+1}^{L-1} C_{L-1}^{|s|} + \sum_{s=-L+w}^{L-w} C_{L-w}^{|s|}}$. Furthermore, according to the assumption that connection length L is independently chosen from a geometric distribution $G(L)$ in Section 3, we have Equation (1). For the same reason, we have Equation (2).

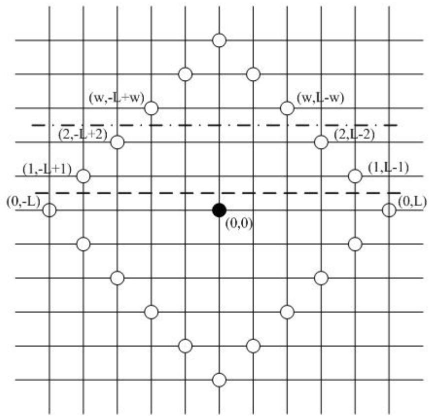

Fig. 4. All the $4L$ endpoints of the connections emanating from or terminating at PE$(0,0)$ with the length of $L = 5$ and the length of hop neighbour connection $w = 3$

Lemma 2: Let $X(U_{nfo})$ and $X(U_{sfo})$ be the number of connections emanating from U_{nfo} and U_{sfo} of PE$(0,0)$. Then, $X(U_{nfo})$ and $X(U_{sfo})$ are independent and Poisson distributed with parameters $P(U_{nfo})\lambda/4$ and $P(U_{sfo})\lambda/4$, respectively.

Proof: $G(L)\frac{\sum_{s=-L+1}^{L-1} C_{L-1}^{|s|}}{\sum_{s=-L+1}^{L-1} C_{L-1}^{|s|}+\sum_{s=-L+w}^{L-w} C_{L-w}^{|s|}} < G(L) < \varepsilon^{L-1}$.When $|\varepsilon| < 1$, geometric progression $\sum_{L=1}^{\infty} \varepsilon^{L-1}$ is convergent, so according to comparison principle, progression $\sum_{L=1}^{\infty} G(L)\frac{\sum_{s=-L+1}^{L-1} C_{L-1}^{|s|}}{\sum_{s=-L+1}^{L-1} C_{L-1}^{|s|}+\sum_{s=-L+w}^{L-w} C_{L-w}^{|s|}}$ is convergent too, which means that $P(U_{nfo})$ is a constant. It is known that the product of a constant and a random variable which is Poisson distributed is also Poisson distributed. Since the number of connections emanating from the upper border of PE$(0,0)$, $X(U)$ is independent and Poisson distributed with parameter $\lambda/4$, $X(U_{nfo}) = P(U_{nfo})X(U)$ is Poisson distributed with parameter $P(U_{nfo})\lambda/4$. For the same reason, $X(U_{sfo})$ is Poisson distributed with parameter $P(U_{sfo})\lambda/4$.

Lemma 3: For a connection x_4, terminating at the upper border of PE$(0,0)$ and emanating from PE(r,s), the probabilities of the events that x_4 uses U_{nfi} and U_{sfi} of PE$(0,0)$ are $P(U_{nfi})$ and $P(U_{sfi})$, respectively. Let $X(U_{nfi})$ and $X(U_{sfi})$ be the number of connections terminating at U_{nfi} and U_{sfi} of PE$(0,0)$. Then, $X(U_{nfi})$ and $X(U_{sfi})$ are independent and Poisson distributed with parameters $P(U_{nfi})\lambda$ and $P(U_{sfi})\lambda$, respectively, where

$$P(U_{nfi}) = \sum_{L=1}^{\infty} G(L)q(L) \sum_{s=-L+1}^{L-1} \frac{C_{L-1}^{|s|}}{C_{L-1}^{|s|} + C_{L-w}^{|s|}} \tag{3}$$

$$P(U_{sfi}) = \sum_{L=1}^{\infty} G(L)q(L) \sum_{s=-L+1}^{L-1} \frac{C_{L-w}^{|s|}}{C_{L-1}^{|s|} + C_{L-w}^{|s|}} \tag{4}$$

where $L = |r| + |s|$, and $C_0^0 = 1$. When $L < w$, $C_{L-w}^{|s|} = 0$.

Proof: As Fig. 1, if x_4 uses U_{nfi} of PE$(0,0)$, it will pass through PE$(1,0)$, and there are $C_{L-1}^{|s|}$ possible paths from PE(r,s) to PE$(1,0)$. Because our stochastic model always chooses the path with the minimal Manhattan distance, PE(r,s) should be above the dash in Fig. 4. Similarly, if x_4 uses U_{sfo} of PE$(0,0)$, it will pass through PE$(w,0)$, and then PE(r,s) should be above the dashdot in Fig. 4. Thereby, there are $C_{L-w}^{|s|}$ possible paths from PE$(w,0)$ to PE(r,s).

All the PEs above the dashdot in Fig.4 can emit connections to U_{nfi} and U_{sfi} of PE$(0,0)$, thus the proportions of the entire possible paths with length L terminating at U_{nfi} and U_{sfi} are $\frac{C_{L-1}^{|s|}}{C_{L-1}^{|s|}+C_{L-w}^{|s|}}$ and $\frac{C_{L-w}^{|s|}}{C_{L-1}^{|s|}+C_{L-w}^{|s|}}$, respectively. Besides, all the PEs between the dash and dashdot in Fig. 4 can only emit connections to U_{nfi} of PE$(0,0)$, and the number of such PEs is $2(w-1)$.

Based on the assumptions that connection length L is independently chosen from a geometric distribution $G(L)$ and the probability of choosing one border of the endpoints is $q(L)$ in Section 3, we have Equation (3). As Lemma 2, $G(L)q(L)\sum_{s=-L+1}^{L-1} \frac{C_{L-1}^{|s|}}{C_{L-1}^{|s|}+C_{L-w}^{|s|}} < G(L)\frac{1}{8L-4}(2L-1) < \frac{1}{4}\varepsilon^{L-1}$, so $P(U_{nfi})$ is a constant. According to another assumption that the number of connections per PE can be drawn independently from a Poisson distribution with parameter

λ in Section 3, $X(U_{nfi})$ is Poisson distributed with parameter $P(U_{nfi})\lambda$. For the same reason, we have Equation (4) and $X(U_{sfi})$ is Poisson distributed with parameter $P(U_{sfi})\lambda$.

Lemma 4: For a connection x_5, emanating from PE(r, s) and terminating at PE$(-t+|h|, -h)$, where $t > 0$, $h = -t, -t+1, \cdots, t-1, t$ and $hs \geq 0$, the probabilities of the events that x_5 uses U_{nci} and U_{sci} of PE$(0,0)$ are $P(U_{nci})$ and $P(U_{sci})$, respectively:

$$P(U_{nci}) = \sum_{L=2}^{\infty} G(L) \sum_{t=1}^{L-1} \sum_{s=-(L-t-1)}^{L-t-1} \sum_{h=-t}^{t} \frac{C_{L-t-1}^{|s|} C_t^{|h|}}{C_L^{|s|+|h|}} q'(L, s, h, t) \quad (5)$$

$$P(U_{sci}) = \sum_{L=w+1}^{\infty} G(L) \sum_{t=1}^{L-w} \sum_{s=-(L-t-w)}^{L-t-w} \sum_{h=-t}^{t} \frac{C_{L-t-w}^{|s|} C_t^{|h|}}{C_L^{|s|+|h|}} q'(L, s, h, t) \quad (6)$$

where, $L = |r| + |s| + t$, $C_0^0 = 1$ and

$$q'(L, s, h, t) = \begin{cases} 0, \ hs < 0 \\ q(L), \ hs \geq 0 \text{ and } (h = 0 \text{ or } h = \pm t) \\ 2q(L), \ \text{others} \end{cases}$$

Proof: If x_5 uses U_{nci} of PE$(0,0)$, it will pass through PE$(1,0)$. For each t, x_5 is divided into three segments: the first is from PE(r,s) to PE$(1,0)$ with length $L-t-1$, the second is from PE$(1,0)$ to PE$(0,0)$ with length 1, and the third is from PE$(0,0)$ to PE$(-t+|h|, -h)$ with length t. Thus, there is $C_{L-t-1}^{|s|} C_t^{|h|}$ possible paths form PE(r,s) to PE$(-t+|h|, -h)$ if x_5 uses U_{nci} of PE$(0,0)$. Since there are $C_L^{|s|+|h|}$ possible paths from PE(r,s) to PE$(-t+|h|, -h)$, taking into account the assumption that the probability of choosing one border of the endpoints is $q(L)$, the probability of using U_{nci} is $\frac{C_{L-t-1}^{|s|} C_t^{|h|}}{C_L^{|s|+|h|}} q(L)$.

As Fig. 5, when the length of x_5 is L, there are $2(L-t-1)+1$ starting points and $2t+1$ endpoints for each t. Not each of the starting points and endpoints can constitute a point-pair which denotes a possible path of x_5 because they have to satisfy that $hs \geq 0$. In addition, when $h = 0$ or $h = \pm t$, x_5 can only terminate at one border of the endpoint, otherwise x_5 can end at two borders of it. Calculating the sum of the probabilities for all point-pairs, we have the probability of using U_{nci} with length L is $\sum_{t=1}^{L-1} \sum_{s=-(L-t-1)}^{L-t-1} \sum_{h=-t}^{t} \frac{C_{L-t-1}^{|s|} C_t^{|h|}}{C_L^{|s|+|h|}} q'(L, s, h, t)$. With the assumption that connection length L is independently chosen from a geometric distribution $G(L)$, we have Equation (5). Because

$$G(L) \sum_{t=1}^{L-1} \sum_{s=-(L-t-1)}^{L-t-1} \sum_{h=-t}^{t} \frac{C_{L-t-1}^{|s|} C_t^{|h|}}{C_L^{|s|+|h|}} q'(L, s, h, t) < G(L) \sum_{t=1}^{L-1} \sum_{s=-(L-t-1)}^{L-t-1} \sum_{h=-t}^{t} 1 \cdot 2q(L)$$

$$= G(L) \sum_{t=1}^{L-1} \frac{1}{4L-2} [2(L-t)-1](2t+1) < G(L) \sum_{t=1}^{L-1} \frac{1}{4L-2} \cdot 2L \cdot 3t$$

$$= (1-\varepsilon)\varepsilon^{L-1} \frac{3L}{2L-1} \frac{L(L-1)}{2} < \varepsilon^{L-1} \frac{3L}{L} \frac{L^2}{2} = \frac{3}{2} \varepsilon^{L-1} L^2 = u(L)$$

and $\lim_{L\to\infty}\frac{u(L+1)}{u(L)} = \lim_{L\to\infty}\varepsilon(1+\frac{1}{L})^2 = \varepsilon < 1$, according to D Alembert discriminance, progression $\sum_{L=1}^{\infty} u(L)$ is convergent. Thereupon, according to comparison principle, progression

$$\sum_{L=2}^{\infty} G(L) \sum_{t=1}^{L-1} \sum_{s=-(L-t-1)}^{L-t-1} \sum_{h=-t}^{t} \frac{C_{L-t-1}^{|s|} C_t^{|h|}}{C_L^{|s|+|h|}} q'(L,s,h,t)$$

is convergent too, which means that $P(U_{nci})$ is a constant.

For the same reason, if x_5 uses U_{sci} of PE$(0,0)$, it will pass through PE$(w,0)$. Then, we have Equation (6) and $P(U_{sci})$ is a constant too.

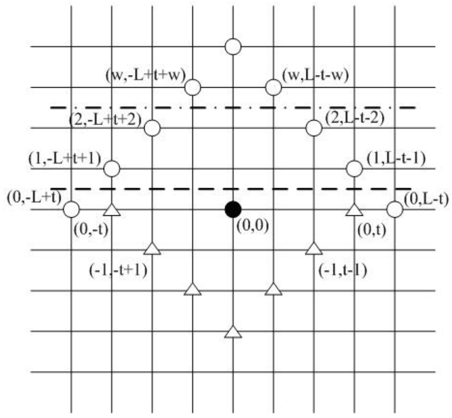

Fig. 5. All the starting points (denoted as circles) and endpoints (denoted as triangles) of the connections traversing PE$(0,0)$ with $L=7$, $w=3$, and $t=3$

Lemma 5: For a connection x_6, emanating from PE(r,s) and terminating at PE$(t-|h|,-h)$, where $t>0$, $h=-t,-t+1,\cdots,t-1,t$ and $hs \geq 0$, the probabilities of the events that x_6 uses U_{nco} and U_{sco} of PE$(0,0)$ are $P(U_{nco})$ and $P(U_{sco})$, respectively:

$$P(U_{nco}) = \sum_{L=2}^{\infty} G(L) \sum_{t=1}^{L-1} \sum_{s=-(L-t)}^{L-t} \sum_{h=-(t-1)}^{t-1} \frac{C_{L-t}^{|s|} C_{t-1}^{|h|}}{C_L^{|s|+|h|}} q''(L,s,h,t), \quad (7)$$

$$P(U_{sco}) = \sum_{L=w+1}^{\infty} G(L) \sum_{t=w}^{L-1} \sum_{s=-(L-t)}^{L-t} \sum_{h=-(t-w)}^{t-w} \frac{C_{L-t}^{|s|} C_{t-w}^{|h|}}{C_L^{|s|+|h|}} q'''(L,s,h,t), \quad (8)$$

where $L=|r|+|s|+t$,

$$q''(L,s,h,t) = \begin{cases} 0, & hs<0 \\ q(L), & hs \geq 0 \text{ and } (h=0 \text{ or } h=\pm(t-1)) \\ 2q(L), & \text{others} \end{cases}$$

and

$$q'''(L,s,h,t) = \begin{cases} 0, & hs < 0 \\ q(L), & hs \geq 0 \text{ and } (h = 0 \text{ or } h = \pm(t-w)) \\ 2q(L), & \text{others} \end{cases}$$

Proof: As Lemma 4.

Lemma 6: Let $X(U_{nci})$, $X(U_{sci})$, $X(U_{nco})$ and $X(U_{sco})$ be the number of connections traversing U_{nci}, U_{sci}, U_{nco} and U_{sco} of PE$(0,0)$, respectively. Their mathematical expectations are:

$$E[X(U_{nci})] = \frac{P(U_{nci})}{P(U_{nci}) + P(U_{sci})} E[X(U_{ci})]$$

$$E[X(U_{sci})] = \frac{P(U_{sci})}{P(U_{nci}) + P(U_{sci})} E[X(U_{ci})]$$

$$E[X(U_{nco})] = \frac{P(U_{nco})}{P(U_{nco}) + P(U_{sco})} E[X(U_{co})]$$

$$E[X(U_{sco})] = \frac{P(U_{sco})}{P(U_{nco}) + P(U_{sco})} E[X(U_{co})],$$

where $X(U_{ci}) = X(U_{nci})+X(U_{sci})$, $X(U_{co}) = X(U_{nco})+X(U_{sco})$ and $E[X(U_{ci})] = E[X(U_{co})] = \frac{\lambda}{4}\frac{\varepsilon}{1-\varepsilon}$.

Proof: The number of PEs that a connection traverses with length L is $X(L) = L - 1$. With the assumption that connection length L is independently chosen from a geometric distribution $G(L) = (1-\varepsilon)\varepsilon^{L-1}$, the mathematical expectation of $X(L)$ is $E[X(L)] = \sum_{L=1}^{\infty} G(L)(L-1) = \frac{\varepsilon}{1-\varepsilon}$. Let n and m be the number of connections in a circuit and the number of PEs in the array, respectively. Thus, the mathematical expectation of the number of connections traversing per PE is $\frac{n}{m}\frac{\varepsilon}{1-\varepsilon} = \lambda\frac{\varepsilon}{1-\varepsilon}$. Since four borders of a PE are chosen with the same probability, we have $E[X(U_{ci})] = E[X(U_{co})] = \frac{\lambda}{4}\frac{\varepsilon}{1-\varepsilon}$.

From Lemma 4, the probabilities of the events that x_5 uses U_{nci} and U_{sci} of PE$(0,0)$ are $P(U_{nci})$ and $P(U_{sci})$, respectively, so the proportion of using U_{nci} is $\frac{P(U_{nci})}{P(U_{nci})+P(U_{sci})}$, and $E[X(U_{nci})] = \frac{P(U_{nci})}{P(U_{nci})+P(U_{sci})} E[X(U_{ci})]$. For the same reason, we have $E[X(U_{sci})]$, $E[X(U_{nco})]$ and $E[X(U_{sco})]$.

5 Estimation and Simulation

It is known that the mathematical expectation of a random variable which is Poisson distributed with parameter λ is λ. Thus, we are able to have $E[X(U_{nfi})]$, $E[X(U_{sfi})]$, $E[X(U_{nfo})]$, $E[X(U_{sfo})]$, $E[X(U_{nci})]$, $E[X(U_{sci})]$, $E[X(U_{nco})]$ and $E[X(U_{sco})]$ from Lemmas 1-6.

Using Lemmas 1 and 2, we have $E[X(U_{nfo}) + X(U_{sfo})] = \frac{\lambda}{4}$. On the other side, we have $E[X(U_{nfi}) + X(U_{sfi})] = \frac{\lambda}{4}$ from Lemma 3. Therefore, the mathematical expectation of the number of connections emanating from the upper border of PE(0, 0) is equal to that of the number of connections terminating at the upper border of it. Additionally, from Lemmas 4 and 5, we have $E[X(U_{nci})] = E[X(U_{nco})]$ and $E[X(U_{sci})] = E[X(U_{sco})]$.

A simulation program is exploited to verify our approach. With the assumptions that the number of connections per PE can be drawn independently from a Poisson distribution with parameter λ, connection length L is independently chosen from a geometric distribution $G(L) = (1-\varepsilon)\varepsilon^{L-1}$, where $\varepsilon \in (0, 1)$, and the probability of choosing one border of the endpoints is $q(L)$, the program routes all the connections with the minimal Manhattan distance and calculates the average number of connections using U_{nfo}, U_{sfo} and so on, such as $\overline{X(U_{nfo})}$ and $\overline{X(U_{sfo})}$. The inputs of the simulation program are n, m, w and ε, where n is the number of connections in the circuit, m is the number of PEs in the array, w is the length of hop neighbour connection, and ε is the parameter of geometric distribution $G(L)$. Table 1 is the results of the simulation program with $w = 2$ and $\varepsilon = 0.3$ [7], and Table 2 is the theoretical estimation using Lemmas 1-6.

Table 1. Simulation results

n	m	$\overline{X(U_{nfo})}$	$\overline{X(U_{sfo})}$	$\overline{X(U_{nfi})}$	$\overline{X(U_{sfi})}$	$\overline{X(U_{nco})}$	$\overline{X(U_{sco})}$	$\overline{X(U_{nci})}$	$\overline{X(U_{sci})}$
251	16	3.53	0.39	3.50	0.42	1.20	0.20	1.23	0.17
319	16	4.34	0.64	4.44	0.55	2.06	0.30	1.97	0.39
479	25	4.21	0.58	4.22	0.57	1.89	0.33	1.88	0.34
688	25	6.15	0.73	6.18	0.70	2.31	0.37	2.28	0.40

Table 2. Theoretical estimation

n	m	$E[X(U_{nfo})]$	$E[X(U_{sfo})]$	$E[X(U_{nfi})]$	$E[X(U_{sfi})]$	$E[X(U_{nco})]$	$E[X(U_{sco})]$	$E[X(U_{nci})]$	$E[X(U_{sci})]$
251	16	3.61	0.31	3.70	0.22	1.41	0.27	1.41	0.27
319	16	4.58	0.40	4.70	0.28	1.79	0.34	1.79	0.34
479	25	4.41	0.38	4.52	0.27	1.72	0.33	1.72	0.33
688	25	6.33	0.55	6.49	0.39	2.47	0.48	2.47	0.48

6 Conclusion

We presented a new stochastic model for mesh-based reconfigurable computing based on the statistical distributions. The average number of each type of connections is estimated, and the simulation results demonstrate the effectiveness of our approach. With our elementary research, designers can estimate the required interconnection resource quickly and optimize their design of PE array accordingly. Incorporating more knowledge from the actual design process, the further research is directed to developing an estimation of other interconnect design parameters such as area occupancy, signal delay, power dissipation, etc.

References

1. A. El Gamal, "Two-dimensional stochastic model for interconnections in master slice integrated circuits," *IEEE Trans. Computer-Aided Design*, Vol. CAD-1, 1981.
2. C. Bobda, and A. Ahmadinia, "Dynamic interconnection of reconfigurable modules on reconfigurable devices," *Design & Test of Computers, IEEE*, Vol. 22, Issue 5, pp. 443 - 451, 2005.
3. R. Miller, V.K. Prasanna-Kumar, D.I. Reisis, and Q.F. Stout, "Parallel computations on reconfigurable meshes," *IEEE Transactions on Computers*, Vol. 42, Issue 6, pp. 678 - 692, 1993.
4. J. Cong, and Z. Pan, "Interconnect performance estimation models for design planning," *IEEE Transactions on Computer-Aided Design of Integrated Circuits and Systems*, Vol. 20, Issue 6, pp. 739-752, 2001.
5. S.D. Brown, J. Rose, and Z.G. Vranesic, "A stochastic model to predict the routability of field-programmable gate arrays," *IEEE Transactions on Computer-Aided Design of Integrated Circuits and Systems*, Vol. 12, Issue 12, pp. 1827 - 1838, 1993.
6. M. Maresca, and P. Baglietto, "A programming model for reconfigurable mesh based parallel computers," *Programming Models for Massively Parallel Computers*, pp. 124-133, 1993.
7. X. Song, Q. Tang, D. Zhou, and Y. Wang, "Wire space estimation and routability analysis," *IEEE Transactions on Computer-Aided Design of Integrated Circuits and Systems*, Vol. 19, Issue 5, pp. 624 - 628, 2000.
8. K. Bondalapati, and V.K. Prasanna, "Reconfigurable computing systems," Proceedings of IEEE, pp. 356 -359, 2002.
9. D.A. Buell, J.M. Arnold, and W. J. Kleinfelder, "FPGAs in a Custom Computing Machine," IEEE Computer Society Press, 1996.
10. J. Vuillemin, P. Bertin, D. Roncin, M. Shand, H. Touati, and P. Boucard, "Programmable Active Memories: Reconfigurable Systems Come of Age," *IEEE Transactions on VLSI Systems*, Vol. 4, No. 1, pp. 56-69, 1996.
11. P. Athanas and A. Abbott, "Real-Time Image Processing on a Custom Computing Platform," *IEEE Computer*, pp. 16-24, 1995.
12. J. Woodfill and B. Von Herzen, "Real-Time Stereo Vision on the PARTS Reconfigurable Computer," *IEEE Symposium on FPGAs for Custom Computing Machines*, 1997.
13. C. Philip , and S. Dirk, "The interpretation and application of Rent's rule," *IEEE Transactions on Very Large Scale Integration (VLSI) Systems*, Vol. 8, No. 6, pp. 639-648, 2000.
14. Z. Dai, and D.K. Banerji, "Routability prediction for Field Programmable Gate Arrays with a routing hierarchy," *VLSI Design*, pp. 85-90, 2003.